Journal of Steroid Biochemistry and Molecular Biology xxx (xxxx) 105874

Contents lists available at ScienceDirect

Journal of Steroid Biochemistry and Molecular Biology

journal homepage: www.elsevier.com/locate/jsbmb

Functional characterization of two 20β-hydroxysteroid dehydrogenase type 2 homeologs from *Xenopus laevis* reveals multispecificity

Janina Tokarz [a,*], Stefan M. Schmitt [b], Gabriele Möller [a], André W. Brändli [b], Jerzy Adamski [a,c,d,e]

[a] Helmholtz Zentrum München, German Research Center for Environmental Health, Research Unit Molecular Endocrinology and Metabolism, Neuherberg, Germany
[b] Walter Brendel Centre of Experimental Medicine, University Hospital and Ludwig-Maximilians-University Munich, Munich, Germany
[c] German Center for Diabetes Research, Neuherberg, Germany
[d] Lehrstuhl für Experimentelle Genetik, Technische Universität München, Freising-Weihenstephan, Germany
[e] Department of Biochemistry, Yong Loo Lin School of Medicine, National University of Singapore, Singapore, Singapore

ARTICLE INFO

Keywords:
Hydroxysteroid dehydrogenase
Cortisone
hsd20b2
20β-reduction
Steroid catabolism
Frog

ABSTRACT

The African clawed frog, *Xenopus laevis*, is a versatile model for biomedical research and is largely similar to mammals in terms of organ development, anatomy, physiology, and hormonal signaling mechanisms. Steroid hormones control a variety of processes and their levels are regulated by hydroxysteroid dehydrogenases (HSDs). The subfamily of 20β-HSD type 2 enzymes currently comprises eight members from teleost fish and mammals. Here, we report the identification of three 20β-HSD type 2 genes in *X. tropicalis* and *X. laevis* and the functional characterization of the two homeologs from *X. laevis*. *X. laevis* Hsd20b2.L and Hsd20b2.S showed high sequence identity with known 20β-HSD type 2 enzymes and mapped to the two subgenomes of the allotetraploid frog genome. Both homeologs are expressed during embryonic development and in adult tissues, with strongest signals in liver, kidney, intestine, and skin. After recombinant expression in human cell lines, both enzymes co-localized with the endoplasmic reticulum and catalyzed the conversion of cortisone to 20β-dihydrocortisone. Both Hsd20b2.L and Hsd20b2.S catalyzed the 20β-reduction of further C_{21} steroids (17α-hydroxyprogesterone, progesterone, 11-deoxycortisol, 11-deoxycorticosterone), while only Hsd20b2.S was able to convert corticosterone and cortisol to their 20β-reduced metabolites. Estrone was only a poor and androstenedione no substrate for both enzymes. Our results demonstrate multispecificity of 20β-HSD type 2 enzymes from *X. laevis* similar to other teleost 20β-HSD type 2 enzymes. *X. laevis* 20β-HSD type 2 enzymes are probably involved in steroid catabolism and in the generation of pheromones for intraspecies communication. A role in oocyte maturation is unlikely.

1. Introduction

The African clawed frog, *Xenopus laevis*, has been used since decades as versatile animal model for biomedical research [1]. Fundamental mechanisms of vertebrate cell and developmental biology have been investigated using this model, such as vertebrate axis formation, cell cycle regulation, cellular reprogramming [2], and biochemical signaling pathways [1]. Further, human embryonic development and the basis for human inherited diseases can be easily studied in wild type and genetically engineered frogs, respectively [1,3]. *X. laevis* are robust aquatic frogs tolerating a wide range of living conditions. Oviposition of comparably large eggs is inducible by injection of human gonadotropin year-round, and the embryos develop externally in simple salt solutions [4]. Being transparent, every developmental stage can easily be monitored or manipulated [1]. The embryos are therefore also amenable for *in vivo* drug screening [1], especially for assessing teratogenicity. Several tools for genetic manipulation, such as morpholinos, transcription activator-like effector nucleases (TALENs), or CRISPR/Cas, are established in *X. laevis* [1]. However, the frog has a paleotetraploid genome (allotetraploidy), which arose by hybridization of two parent species at around 17–18 million years ago [5]. Due to functional redundancy, loss or silencing of genes occurred since then, but more than 56 % of genes were retained as duplicates [5]. These duplicates on individual subgenomes (designated as 'L' and 'S') are termed home-

* Corresponding author at: Helmholtz Zentrum München, German Research Center for Environmental Health, Research Unit Molecular Endocrinology and Metabolism, Ingolstaedter Landstrasse 1, 85764, Neuherberg, Germany.
E-mail address: janina.tokarz@helmholtz-muenchen.de (J. Tokarz).

https://doi.org/10.1016/j.jsbmb.2021.105874
Received 16 December 2020; Received in revised form 25 February 2021; Accepted 9 March 2021
0960-0760/

ologs [1,5]. In contrast, the closely related Western clawed frog *Xenopus tropicalis* has a true diploid genome [1,5].

Amphibians have a common evolutionary history with mammals that is estimated to be 100 million years longer than for example between zebrafish (*Danio rerio*) and mammals [6]. This results in broad synteny at the genome level and in large similarities in organ development, anatomy, and physiology [6,7]. Furthermore, *X. laevis* share identical hormones, conserved receptors, and conserved mechanisms of gene regulation with other vertebrate counterparts [8–10]. This also holds true for steroid hormone signaling, rendering *X. laevis* a frequently used model organism to study endocrine disruption [11–13] or the mechanism of action of steroid metabolism disruption [14].

Steroids control a variety of vital processes, such as development, reproduction, metabolism, salt and water balance, immune responses [15], as well as metamorphosis in amphibians [16]. Steroid biosynthesis as well as pre- and post-receptor metabolism are processes tightly regulated by enzymes from different families, among which the hydroxysteroid dehydrogenases (HSDs) are very important. HSDs perform oxidations and reductions of hydroxyl- or ketogroups at positions C3, C11, C17, or C20 of the steroid backbone and thereby regulate the interconversion of active and inactive hormones [17]. One group of the enzymes acting on the C20 position of steroids is the subfamily of 20β-HSD type 2 enzymes, which consists currently of eight members, six from teleost fish species (zebrafish, guppy, rainbow trout, tilapia, Japanese eel, and orange spotted grouper) and two from mammals (sheep and cattle) [18–20]. The level of characterization varies largely between the 20β-HSD type 2 members. Zebrafish 20β-HSD type 2 catalyzes the efficient reduction of cortisone to 20β-dihydrocortisone [18] and is involved together with 11β-HSD type 2 in the catabolism of the stress hormone cortisol [21]. Both enzymes are ubiquitously expressed in zebrafish and are upregulated upon cortisol treatment or a physiological stressor [18,21]. 20β-Dihydrocortisone activated neither the glucocorticoid nor the mineralocorticoid receptor, but was found in large quantities in both free and conjugated form in zebrafish holding water [21]. This evidence supported the conclusion of 20β-HSD type 2 being involved in cortisol catabolism and excretion. Recently, we established that 20β-HSD type 2 from zebrafish, tilapia, rainbow trout, guppy, sheep, and cattle are multispecific enzymes, which catalyze the conversion of a plethora of C_{21} steroids *in vitro*, implying further physiological roles for this enzyme family [22]. Interestingly, the 20β-HSD type 2 from Japanese eel catalyzed the conversion of 11-ketoandrostenedione to 11-ketotestosterone *in vitro* and was ubiquitously expressed with stronger signals in liver, pituitary, and testis [19]. Yet, Japanese eel 20β-HSD type 2 is probably not involved in testicular 11-ketotestosterone formation, because its mRNA was not regulated upon gonadotropin stimulation [19]. The surprising 17β-hydroxysteroid dehydrogenase activity of Japanese eel 20β-HSD type 2 with androgens was not observed for other teleost 20β-HSD type 2 enzymes with the substrate androstenedione [18,22]. Further putative 20β-HSD type 2 members in spotted gar, fugu, medaka, stickleback, and common carp were identified [20,23] but so far not characterized.

In this study, we expanded the family of 20β-HSD type 2 enzymes by identifying two 20β-HSD type 2 homeologs in the genome of *X. laevis* and one ortholog in the genome of *X. tropicalis*. To understand their physiological role, we performed a functional characterization of the *X. laevis* enzymes including expression analysis during frog embryonic development and in adult tissues, subcellular localization analysis, and analysis of their substrate specificities using a panel of C_{21} steroids as well as androstenedione and estrone as substrates.

2. Methods

2.1. Identification, analysis, and annotation of sequences

To identify 20β-HSD type 2 members in the genome of *X. laevis* and *X. tropicalis*, BLAST searches in EST and Nucleotide Collection databases at the NCBI were performed using the zebrafish 20β-HSD type 2 coding sequence as query. Sequences were considered suitable for further analysis if they had a certain quality (more than 40 % identity at alignment with the query sequence). Strongly truncated sequences were removed from the analysis. Accession numbers of all sequences extracted are listed in Supplementary Table 1.

For phylogenetic analysis, the identified *Xenopus* candidate sequences were combined with known RNA and protein sequences of the 20β-HSD type 2, 17β-HSD type 12, and 17β-HSD type 3 enzyme families from teleost fishes and mammals, which were characterized in our previous work [18]. Multiple alignment of protein sequences was conducted using Blosum matrix and calculation of phylogenetic trees with MEGA7 software [24] applying the Neighbor-Joining method [25]. For testing of inferred phylogeny, a bootstrapping with 1000 replications was performed [26].

To identify the location of the identified 20β-HSD type 2 homeologs in the sub-genomes of *X. laevis*, BLAST analyses were carried out at Xenbase (http://www.xenbase.org/, RRID:SCR_003280) [27]. For this, the *X. laevis* candidate RNA sequences were compared to *Xenopus laevis* J-strain 9.2 Genome using default parameters.

Protein sequence alignments were generated using Clustal Omega (https://www.ebi.ac.uk/Tools/msa/clustalo/). Pairwise protein sequence identities in % were determined using the BLAST 2 Sequences algorithm at the NCBI [28,29].

2.2. Animal husbandry and tissue collection

All animal experiments were performed according to German legislation for the protection of animals and approved by the Regierung von Oberbayern, München, Germany. For *X. laevis* frogs, husbandry and breeding protocols were approved under the permit # 55.2-1-54-2532.0-95-2014. Adult frogs were kept in tanks with tap water at 18 °C and 12 h light/dark cycles. *In vitro* fertilizations, culture, and anesthesia of *X. laevis* embryos was performed as described previously [30]. Developmental stages were determined according to [31]. Embryos were kept in 0.1 x MMR culture medium (0.1 M NaCl, 2 mM KCl, 1 mM $MgSO_4$, 2 mM $CaCl_2$, 5 mM HEPES, pH 7.8) at 22 °C. Embryos were collected at developmental stages 0 (unfertilized eggs, 0 min post fertilization (pf)), 5 (16-cell, 2 h 45 min pf), 8 (blastula, 5 h pf), 10.5 (gastrula, 11 h pf), 20 (neurula, 22 h pf), 30 (tailbud, 1.5 days pf), 40 (tadpole, 2 days 18 h pf), and 45 (swimming tadpole, 4 days pf), with four embryos per sample for all stages up to stage 10.5, three embryos per sample for stages 20 and 30, and two embryos per sample for stages 40 and 45. Culture medium was removed and the embryos were snap-frozen in liquid nitrogen. For tissue preparation from adults, the animals were anesthetized for 45 min in ice-cold water and killed by decapitation. Dissected tissues (brain, eyes, liver, kidney (including the adrenal gland), gonads, muscle, spleen, skin, heart, adipose tissue, intestine, and lung) of both sexes as well as oocytes from the females were rinsed with PBS and snap-frozen in liquid nitrogen.

2.3. Isolation of total RNA

Frozen tissue and embryo samples were kept on dry ice until the addition of 2-3 mL and 1 mL TRIzol reagent (Invitrogen), respectively. The samples were homogenized using a rotor-stator (Heidolph Type DIAX900). Total RNA was extracted by the addition of 0.2 volumes of chloroform, vortexing for 15 s, incubation at room temperature for 3 min, and centrifugation at 4 °C and 21,900 × g for 15 min. The su-

pernatant was transferred to a fresh tube and mixed with 0.53 volumes of 100 % ethanol. This mixture was applied to columns of the RNeasy Midi Kit (Qiagen) and RNA was further purified including a DNase I digestion step according to the manufacturer's protocol. Amount and purity of isolated RNA was assessed using spectrophotometry (NanoDrop ND-1000, ThermoFisher) prior to addition of 40 U RNase inhibitor (Invitrogen). RNA was stored at −80 °C until use.

2.4. Cloning of candidate sequences

1 μg of total RNA isolated from kidney of male *X. laevis* was reverse transcribed into cDNA using the oligo-dT_{18} primer and the RevertAid First Strand cDNA Synthesis Kit (ThermoScientific) according to the manufacturer's protocol. Both 20β-HSD type 2 candidate sequences were amplified by PCR using standard protocols. For primer sequences refer to Supplementary Table 3. The obtained open reading frames were cloned into the vector pDONR201 (Invitrogen) using the Gateway Technology, verified by sequencing, and subcloned into modified pcDNA-DEST vectors (pcDNAmyc/DEST and pDEST-530) [18] resulting in N-terminally and C-terminally tagged constructs, respectively. N-terminally myc-tagged constructs were Hsd20b2.L_pcDNAmyc/DEST and Hsd20b2.S_pcDNAmyc/DEST, and C-terminally myc-tagged constructs were Hsd20b2.L_pDEST-530 and Hsd20b2.S_pDEST-530.

2.5. Expression analysis by RT-PCR

500 ng each of total RNA isolated from different tissues and embryonic stages were reverse transcribed using the oligo-dT_{18} primer and the RevertAid First Strand cDNA Synthesis Kit (ThermoScientific) according to the manufacturer's protocol. For RT-PCR, 1 μL cDNA was added to a total volume of 20 μL PCR reaction mix containing 1.5 mM $MgCl_2$, 0.2 mM dNTPs, 0.5 μM primer, and 0.3 μL lab-made *Taq* polymerase. PCR reactions were run on a RoboCycler (Stratagene) with 1 cycle 5 min at 95 °C, 35 cycles 45 s at 95 °C, 45 s at 54 °C, and 90 s at 72 °C, and 1 cycle 90 s at 72 °C. PCR products were separated on 1% agarose gels. β-Actin controls were included as control reactions. For primer sequences refer to Supplementary Table 3.

2.6. Cell culture

For subcellular localization analyses, the human cervix carcinoma cell line HeLa was maintained in MEM medium (Gibco) supplemented with 10 % fetal bovine serum (FBS Superior; Biochrom) at 37 °C and 5% CO_2 in a humidified atmosphere. For enzyme activity assays, the human embryonic kidney cell line HEK293 was cultivated in DMEM medium (Gibco) supplemented with 10 % fetal bovine serum (FBS Superior; Biochrom) at 37 °C and 5% CO_2 in a humidified atmosphere. The cells were frequently checked to be free of mycoplasma contamination using the MycoAlert™ mycoplasma detection kit (Lonza) and the MycoAlert™ assay control set (Lonza).

2.6.1. Subcellular localization studies

5×10^4 HeLa cells were seeded per well in 6-well plates containing glass coverslips. After 24 h, the cells were transiently transfected with 500 ng of expression plasmid encoding the respective 20β-HSD type 2 and 500 ng of the plasmid pDsRed2-ER (Clontech) for staining the endoplasmic reticulum. Transfection was done using XtremeGENE 9 Transfection Reagent (Roche) according to the manufacturer's instructions and the cells were studied after an incubation time of 24 h. Cells were washed twice with PBS and fixed by incubation for 10 min in PBS containing 3.7 % formaldehyde at growth conditions. For detection of myc-tagged fusion proteins, cells were permeabilized with 0.5 % Triton-X100 in PBS for 5 min at room temperature (RT). After washing the cells twice with PBS, unspecific binding sites were blocked by incubation of the cells in 3 % BSA in PBS for 30 min at RT. Immunochemical detection of the myc-tag was conducted by incubating the cells with primary (monoclonal mouse-anti-C-Myc (9B11); dilution 1:1,000; Cell Signaling) and secondary (Alexa Fluor 488 goat-anti-mouse; dilution 1:2,000; Molecular Probes) antibodies in 3 % BSA in PBS for 1 h each at RT. After washing the cells twice with PBS, counterstaining of the nucleus was performed by incubating the cells for 2 min at RT in PBS containing Hoechst 33342 (Invitrogen) diluted 1:5,000. Cells were washed twice with PBS, mounted on slides with VectaShield mounting medium (VectorLabs) and examined with an Axiophot epifluorescence microscope (Zeiss) using a 63× oil immersion objective. Three channel optical data were collected with the AxioCam MRm camera (Zeiss) and the software AxioVision Rel. 4.6 (Zeiss). Pearson's coefficients of colocalization were determined using the Colocalization Finder plug-in for ImageJ software on 10 pictures per analyzed construct.

2.6.2. Recombinant expression of 20β-HSD type 2 homeologs for enzyme assays and kinetic analyses

For testing the enzymatic activity with several substrates, the plasmids coding for the C-terminally myc-tagged 20β-HSD type 2 homeologs (Hsd20b2.L_pDEST-530 and Hsd20b2.S_pDEST-530) were transfected into HEK293 cells. For each of the two expression plasmids, several T75 flasks (3-8) of cells were transfected with 10 μg plasmid per flask using the XtremeGENE 9 Transfection Reagent (Roche) according to the manufacturer's instructions. 48 h post transfection, cells were harvested by trypsination and washed twice with PBS. From each individual flask, an aliquot of 320 μL was separately collected and stored at −80 °C for expression analysis by Western Blot. Afterwards, the remaining cells transfected with the same plasmid were pooled and split into aliquots containing 600 μg of total protein. The total protein content was determined by the Bradford assay (Bio-Rad) using BSA as reference protein [32]. Cell aliquots were stored at −80 °C until further use.

2.7. Confirmation of recombinant protein expression

Cell aliquots of transfected and untransfected HEK293 cells from pooled cell batches containing 600 μg total protein were resuspended in 300 μL H_2O containing protease inhibitor (Pierce). Cell aliquots of transfected and untransfected HEK293 cells collected from single cell culture flasks (320 μL aliquots) were resuspended in 100 μL H_2O containing protease inhibitor. Resuspended cells were lysed by sonication (6 cycles 15 s in sonication bath, 15 s on ice), and DNA was digested by Benzonase (Sigma). Lysates were centrifuged at 700 × g and 4 °C for 10 min and the supernatants discarded. The pellets were resuspended in 150 μL (for samples originally containing 600 μg total protein) or in 75 μL (for samples collected from individual cell culture flasks) H_2O with protease inhibitor and the protein concentration was determined by the Bradford assay (Bio-Rad) using BSA as reference protein [32]. Subsequently, samples were mixed with Laemmli buffer and heated to 95 °C for 15 min. 10 μg of total protein per sample were separated by SDS-PAGE (10 % polyacrylamide gels) and transferred to a polyvinylidene difluoride (PVDF) membrane (Millipore). The membrane was blocked in Odyssey Blocking Buffer (Li-Cor) diluted 1:1 with PBS for 2 h at room temperature and incubated over night at 4 °C with the polyclonal rabbit-anti-β-actin antibody (A2066; dilution 1:1,000; Sigma) and the monoclonal mouse-anti-C-myc antibody (9B11; dilution 1:200; Cell Signaling) in Odyssey Blocking Buffer diluted 1:1 in 0.05 % Tween-20 in PBS. After three washing cycles with 0.05 % Tween-20 in PBS, the membrane was incubated with the secondary antibodies goat-anti-mouse IRDye 800CW and goat-anti-rabbit IRDye 680RD (dilution 1:20,000; Li-Cor) in Odyssey Blocking Buffer diluted 1:1 in 0.05 % Tween-20 in PBS for 2 h at room temperature. The signals were detected with the Odyssey infrared imaging system (Li-Cor).

2.8. Enzyme activity assays

2.8.1. Determination of enzyme activity with ^{3}H-labeled cortisone

For enzymatic assays with tritiated cortisone, cell aliquots containing 600 μg total protein were resuspended in 500 μL reaction buffer (100 mM NaP_i pH 7.3, 1 mM EDTA, 0.05 % BSA). Reactions consisted of 140 μg total protein in 350 μL reaction buffer and 1 μL tritiated cortisone (cortisone [1,2-^{3}H], final concentration 20 nM; American Radiolabeled Chemicals). Reactions were started by the addition of 150 μL NADPH (final concentration 600 μM; Serva) and incubated at 23 °C for 15 min with gentle shaking. The reactions were terminated by the addition of 100 μL stop solution (0.21 M ascorbic acid, 1% acetic acid (v/v) in methanol). Untransfected HEK293 cells were used as controls. Reactions were performed in triplicates. Steroids were extracted by solid phase extraction (SPE) using Strata C18-E reverse phase cartridges (100 mg/1 mL; Phenomenex) on a vacuum manifold (Varian sample preparation 20 place manifold). The cartridges were activated with two times 1 mL methanol and equilibrated with two times 1 mL water. After the application of the sample, the cartridges were washed with 500 μL water. Steroids were eluted with two times 300 μL methanol and eluates collected in vials. Steroids were analyzed by HPLC System Gold (Beckman-Coulter) using a Reverse Phase Luna 5 μm C18 column (125 × 4 mm I.D., particle size 5 μm; Phenomenex) with 40 % methanol (v/v) in water as running solvent coupled to online-scintillation counter LB 506 D (Berthold). Conversion rates in percent were obtained after integration of the substrate and product peak in the chromatogram with the 24Karat software (Beckman-Coulter).

2.8.2. Determination of steady-state kinetic parameters

For kinetic analyses, aliquots containing 600 μg total protein were resuspended in 250 μL or 600 μL reaction buffer for Hsd20b2.L or Hsd20b2.S, respectively. 140 μg and 600 μg of total protein per reaction were used for Hsd20b2.S and Hsd20b2.L, respectively. Unlabeled cortisone was added (0.54–40.04 μM for Hsd20b2.L and 0.12–7.54 μM for Hsd20b2.S). To monitor cortisone conversion, 20 nM tritiated cortisone (American Radiolabeled Chemicals) was added to each reaction, and reactions were started by the addition of NADPH (final concentration 600 μM) in a total reaction volume of 500 μL. Assays were performed in triplicates. Samples were incubated at 23 °C with gentle shaking for 15 min and 30 min for 20β-HSD type 2.S and 20β-HSD type 2.L, respectively. Reactions were terminated by adding 100 μL stop solution. Steroid extraction by SPE, separation by HPLC, and peak integration was performed as described above. For the calculation of kinetic parameters, the percentages of substrate conversion were converted into pmol min^{-1} mg^{-1} total protein and the resulting values were taken as initial velocities. Michaelis-Menten kinetics were calculated by non-linear fitting using the Enzyme Kinetics 1.3 add-on for SigmaPlot 12.0 (Systat Software Inc.).

2.8.3. Screen for additional substrates by LC-MS/MS

To screen the *X. laevis* 20β-HSD type 2 homeologs for other substrates than cortisone, samples were prepared for liquid chromatography-tandem mass spectrometry (LC-MS/MS). Cell aliquots containing 600 μg total protein were resuspended in 600 μL reaction buffer. Reactions consisted of 200 μg total protein in 890 μL reaction buffer and 10 μL steroid in methanol (stock solutions were concentrated as follows: 200 ng/mL progesterone, 200 ng/mL 11-deoxycorticosterone, 400 ng/mL corticosterone, 200 ng/mL 17α-hydroxprogesterone, 300 ng/mL 11-deoxycortisol, 600 ng/mL cortisol, 200 ng/mL androstenedione, or 300 ng/mL estrone). Final substrate concentrations in the reaction were as follows: 6.36 pM progesterone, 6.05 pM 11-deoxycorticosterone, 11.55 pM corticosterone, 6.05 pM 17α-hydroxyprogesterone, 8.66 pM 11-deoxycortisol, 16.55 pM cortisol, 6.98 pM androstenedione, and 11.09 pM estrone. Steroid concentrations were chosen to be in the physiological range. Reactions were started by the addition of 100 μL NADPH (final concentration 600 μM) and incubated at 23 °C for 1 h with gentle shaking. The reactions were terminated by the addition of 200 μL stop solution. Control reactions contained either untransfected cells (200 μg total protein of untransfected HEK293 cells, 10 μL of the respective steroid stock solution, and 600 μM NADPH) or only 10 μL of the respective steroid stock solution (input control) in a total volume of 1 mL reaction buffer. Every reaction was performed in triplicates.

For quantification of steroids, calibrator working solutions for glucocorticoids and androgens with different steroid concentrations were prepared in triplicates as described previously [22]. Calibrator working solutions for estrone and estradiol (for concentrations of calibrator stock solutions see Supplementary Table 4) were prepared similarly. Addition of internal standard 13C-cortisol (Hydrocortisone-2,3,4-$^{13}C_3$; SigmaAldrich) to all samples was performed as described previously [22]. Extraction of glucocorticoids and androgens by SPE, steroid separation by liquid chromatography, steroid analysis by tandem mass spectrometry (MRM-based detection), and steroid quantification was performed as described previously [22]. Samples containing estrogens were extracted by SPE and evaporated to dryness as described previously [22]. The extracts were reconstituted in 1 mL 25/75 methanol/water (v/v). Liquid chromatography and analysis of estrogens by tandem mass spectrometry was done using the LC-MS/MS method of the Stero*IDQ* kit (Biocrates) [33] with addition of the mass spectrometrical parameters for the internal standard 13C-cortisol as in [22].

3. Results

Zebrafish 20β-HSD type 2 efficiently catalyzes the reduction of cortisone to 20β-dihydrocortisone [18] and plays a vital role in the catabolism of the stress hormone cortisol [21]. Recently, we demonstrated substrate multispecificity for several members of the 20β-HSD type 2 family, which might imply additional physiological roles for the enzymes [22]. Here, we identified three novel members of the 20β-HSD type 2 family in the genomes of *X. laevis* and *X. tropicalis*. The two *X. laevis* homeologs were characterized in detail to understand their physiological role.

3.1. Phylogenetic studies identify 20β-HSD type 2 orthologs in the X. laevis and X. tropicalis genome

To identify potential candidates for 20β-HSD type 2 orthologs in the genome of *X. laevis* and *X. tropicalis*, BLAST searches using both RNA and protein sequence of zebrafish 20β-HSD type 2 (KM279631) as input templates were performed. The search returned five *X. laevis* sequences with more than 44 % identity on the protein level, namely XM_018253819, NM_001092608, NM_001086586, NM_001094901, and XM_018259182. For *X. tropicalis*, we found two sequences, namely XM_002941820 and NM_001017234. Since 20β-HSD type 2 enzymes are closely related to 17β-HSDs type 3 and 12 and novel family members cannot be annotated based on sequence identity alone [18], we performed phylogenetic analysis to determine which *Xenopus* candidate sequence belongs to which enzyme family. In Neighbor Joining analysis, two of the *X. laevis* sequences (NM_001092608 and XM_018253819) clustered together with the 20β-HSD type 2 cluster, two other sequences were found in the 17β-HSD type 12 cluster (NM_001086586 and NM_001094901), and one sequence in the 17β-HSD type 3 cluster (XM_018259182) (Fig. 1). For *X. tropicalis*, one sequence each clustered with the 20β-HSD type 2 (XM_002941820) and the 17β-HSD type 12 cluster (NM_001017234) (Fig. 1). Despite a high sequence identity between 20β-HSD type 2, 17β-HSD type 12, and 17β-HSD type 3 enzymes, all three families cluster separately. The separation of all three groups was supported by high bootstrap values.

To identify the location of the novel 20β-HSD type 2 homeologs in the sub-genomes of *X. laevis*, BLAST analyses at Xenbase [27] were car-

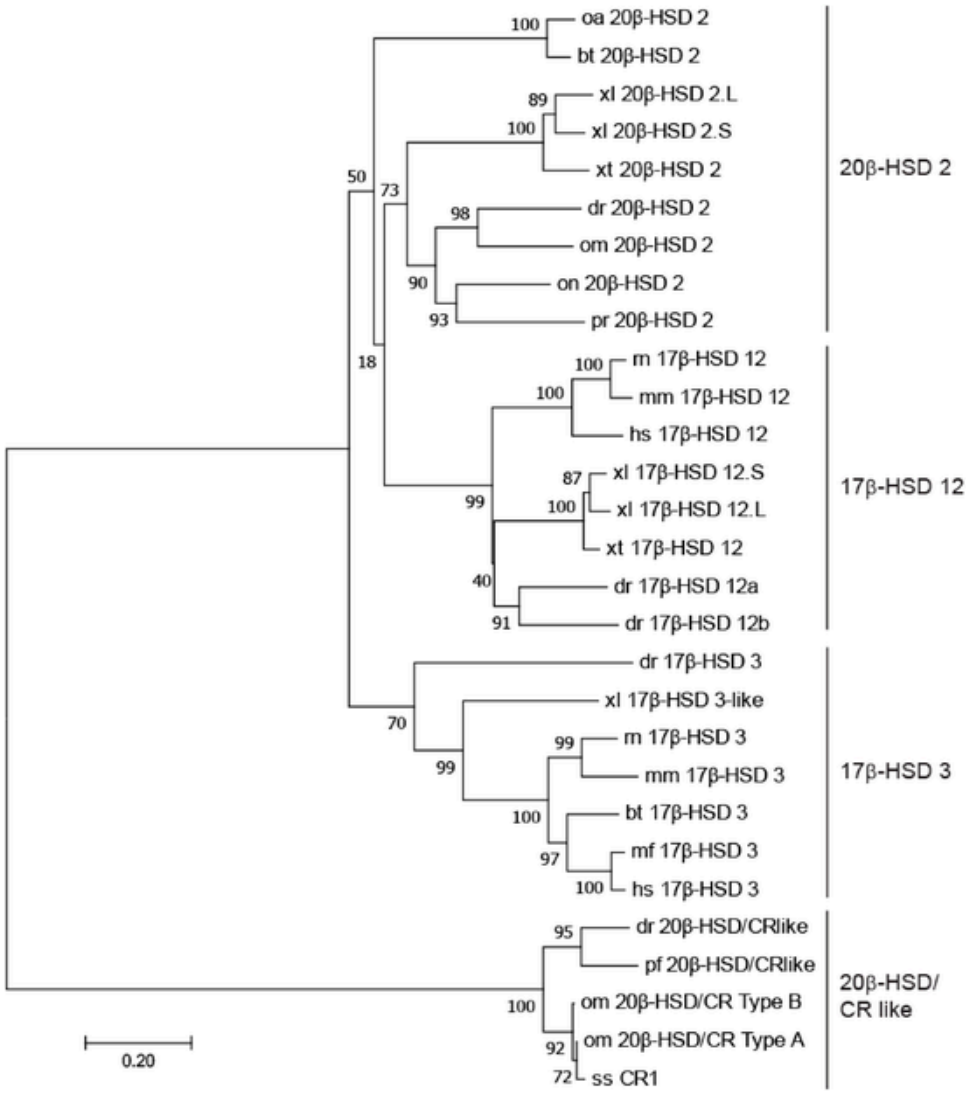

Fig. 1. By phylogenetic analysis, the HSD family membership of five *X. laevis* and two *X. tropicalis* protein sequences was elucidated, which revealed three new members of the 20β-HSD type 2 family. The tree was constructed using the Neighbor Joining method. The percentage of replicate trees in which the associated sequences clustered together in the bootstrap test with 1000 replications are given in percent at the individual dichotomy. Accession numbers can be found in Supplementary Table 1. Species abbreviations: bt, *Bos taurus*; dr, *Danio rerio*; hs, *Homo sapiens*; mf, *Macaca fasciularis*; mm, *Mus musculus*; oa, *Ovis aries*; om, *Oncorhynchus mykiss*; on, *Oreochromis niloticus*; pr, *Poecilia reticulata*; rn, *Rattus norvegicus*; ss, *Salmo salar*; tf, *Tachysurus fulvidraco*; xl, *Xenopus laevis*; xt, *Xenopus tropicalis*.

ried out. Both candidate sequences (NM_001092608 and XM_018253819) mapped to the Xenbase Genepage-5863530. The first candidate sequence NM_001092608 is identical to Xenbase Gene-ID XB-GENE-17340570 and is located on chromosome 3.L. We named this enzyme 20β-HSD type 2.L (gene symbol *hsd20b2.L*, protein symbol Hsd20b2.L). The second candidate sequence XM_018253819 is identical to Xenbase Gene-ID XB-GENE-5863565 and is located in Scaffold 20. We named this enzyme 20β-HSD type 2.S (gene symbol *hsd20b2.S*, protein symbol Hsd20b2.S). The candidate sequence XM_002941820 from *X. tropicalis* is identical to Xenbase Gene-ID XB-GENE-5863531 and is located on chromosome 3. We named the enzyme 20β-HSD type 2 (gene symbol *hsd20b2*, protein symbol Hsd20b2).

Pairwise protein sequence identities between enzymes from all three HSD families 20β-HSD type 2, 17β-HSD type 12, and 17β-HSD type 3 were very high (> 38.3 %; Supplementary Table 2), thus underlining a high degree of identity between the enzymes. All previously characterized 20β-HSD type 2 enzymes, including the novel orthologs from *X. laevis* and *X. tropicalis*, share 45–91 % amino acid residue identity (Supplementary Table 2). In addition, within the group of 17β-HSD type 12 and type 3 enzymes, a very high degree of amino acid residue identity can be observed (58–93 % and 44–94 %, respectively). The pairwise sequence identity between 20β-HSD type 2 and 17β-HSD type 12 members (42–51 %) as well as between 20β-HSD type 2 and 17β-HSD type 3 enzymes (38–48 %) was also very high compared to sequence identities commonly observed for SDR enzymes of unrelated families (~ 15–30 %) [34].

The sequence comparison of the *X. laevis* homeologs Hsd20b2.L and Hsd20b2.S as well as the *X. tropicalis* ortholog Hsd20b2 with zebrafish 20β-HSD type 2 revealed a high degree (52.9–57.7 % identity) of conservation (Fig. 2). *X. tropicalis* 20β-HSD type 2 has a longer N-terminus than the other sequences. Further differences are mostly present in the C-termini of the sequences, which are also of different lengths. The typical conserved residues characteristic for SDR family members, such as the TGxxxGxG motif for cofactor binding or the S-Y-K motif in the active site, are well conserved in all three *Xenopus* 20β-HSD type 2 orthologs (Fig. 2). *X. laevis* homeologs Hsd20b2.L and Hsd20b2.S share 87.0 % sequence identity (including only identical residues) and 91.6 %

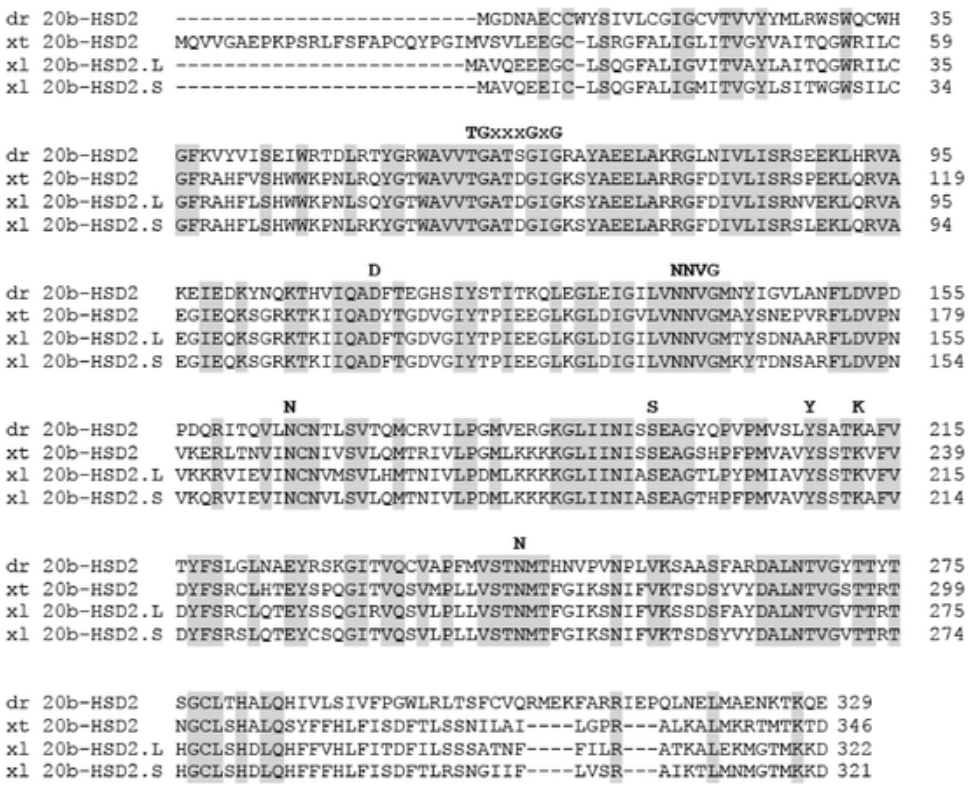

Fig. 2. Sequence comparison of the two *X. laevis* homeologs and the *X. tropicalis* ortholog of 20β-HSD type 2 with the zebrafish enzyme show a high degree of identity between the sequences. Clustal Omega was used for construction of the sequence alignment. Amino acid residues are in single letter code. Identical residues in all sequences are shaded in gray. Amino acid residues belonging to typical SDR motifs are depicted in bold above the alignment. Species abbreviations: dr, *Danio rerio*; xl, *Xenopus laevis*; xt, *Xenopus tropicalis*.

sequence similarity (including residues with similar physicochemical properties and identical residues).

3.2. mRNA expression analyses of 20β-HSD type 2 homeologs in X. laevis

We investigated the expression pattern of the two *X. laevis* 20β-HSD type 2 homeologs by performing RT-PCR in embryos of different stages and in different adult tissues (Fig. 3). RT-PCR instead of qPCR was chosen due to tissue sample limitations. We observed different expression pattern for *hsd20b2.L* and *hsd20b2.S*. During embryonic development, *hsd20b2.L* expression started at stage 10.5 and remained on a constant level from stage 20 to stage 45. *Hsd20b2.S* expression was detectable already at stage 0, but declined during stage 5 and 8. Afterwards, the *hsd20b2.S* expression was visible with slightly variable intensity (Fig. 3). In adults, sex differences were observed in expression for both *hsd20b2.L* and *hsd20b2.S*. *Hsd20b2.L* was generally expressed in more tissues than *hsd20b2.S*. In females, *hsd20b2.L* was expressed in high levels in liver, kidney (including the adrenal gland), eyes, skin, and intestine, while in males such strong signals were only observed in eye, intestine, and skin. Moderate expression of *hsd20b2.L* was found in female ovary, spleen, and oocytes, and in male liver and kidney (including the adrenal gland). Slight expression of *hsd20b2.L* in both sexes was observed in lung and brain as well as in female spleen and heart. In contrast, *hsd20b2.S* showed expression in fewer tissues and this in both sexes. The transcript was expressed in both female and male kidney, eye, and intestine as well as in female skin (Fig. 3). The separate expression of *hsd20b2.L* and *hsd20b2.S* in kidney and adrenal gland was not determined, because the adrenal gland being very close to the anterior medial border of the kidney was not dissected separately.

3.3. Subcellular localization studies

Since 20β-HSD type 2 enzymes from several fish species were co-located with the endoplasmic reticulum (ER) [18], we hypothesized that 20β-HSD type 2 enzymes from *Xenopus* would co-localize with the ER as well. Heterologous expression of the *X. laevis* 20β-HSD type 2 homeologs in HeLa cells showed that both proteins indeed co-localized with the ER (Fig. 4). We obtained high Pearson's correlation coefficients for co-localization of the respective 20β-HSD type 2 enzymes with the marker for the endoplasmic reticulum (Fig. 4) supporting the expected co-localization. The N- or C-terminal position of the myc-tag on the expressed proteins had no influence on the localization of the protein.

3.4. Determination of enzymatic activity and kinetic parameters with the substrate cortisone

20β-HSD type 2 enzymes from teleost fish convert cortisone to 20β-dihydrocortisone, although with different catalytic efficiencies [18,22]. We assumed the *Xenopus* 20β-HSD type 2 to be able to catalyze the same reaction and tested this hypothesis on the two *X. laevis* homeologs. Using similar amounts of total protein of transfected HEK293 cells expressing Hsd20b2.L and Hsd20b2.S, we observed that both homeologs indeed catalyzed cortisone conversion (Fig. 5 A). Hsd20b2.S converted more cortisone than Hsd20b2.L under the given reaction conditions, although expression levels of Hsd20b2.S were lower than those of Hsd20b2.L as shown by Western Blot analysis (Fig. 5 B). We observed no side products beside the substrate and product in all analytical runs.

Determination of kinetic parameters revealed that both enzymes catalyzed the conversion of cortisone with different apparent velocities, because their apparent K_M values differed from another (Table 1). The related Michaelis-Menten kinetics are shown in Supplementary

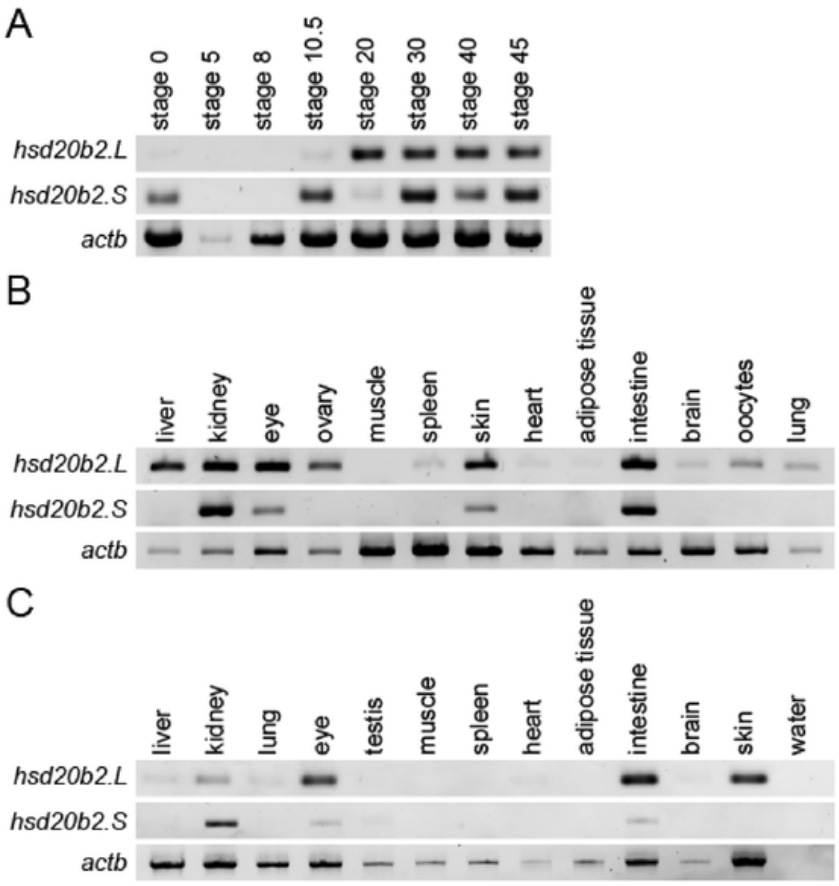

Fig. 3. Expression pattern of the two *X. laevis* 20β-HSD type 2 homeologs differs between the sexes. RT-PCR was performed to analyze the expression pattern of both homeologs during embryogenesis (A), in adult female tissues (B), and in adult male tissues (C). Representative gel photographs show the observed RT-PCR signals for *hsd20b2.L*, *hsd20b2.S*, as well as for *actb*, which was included for control reactions.

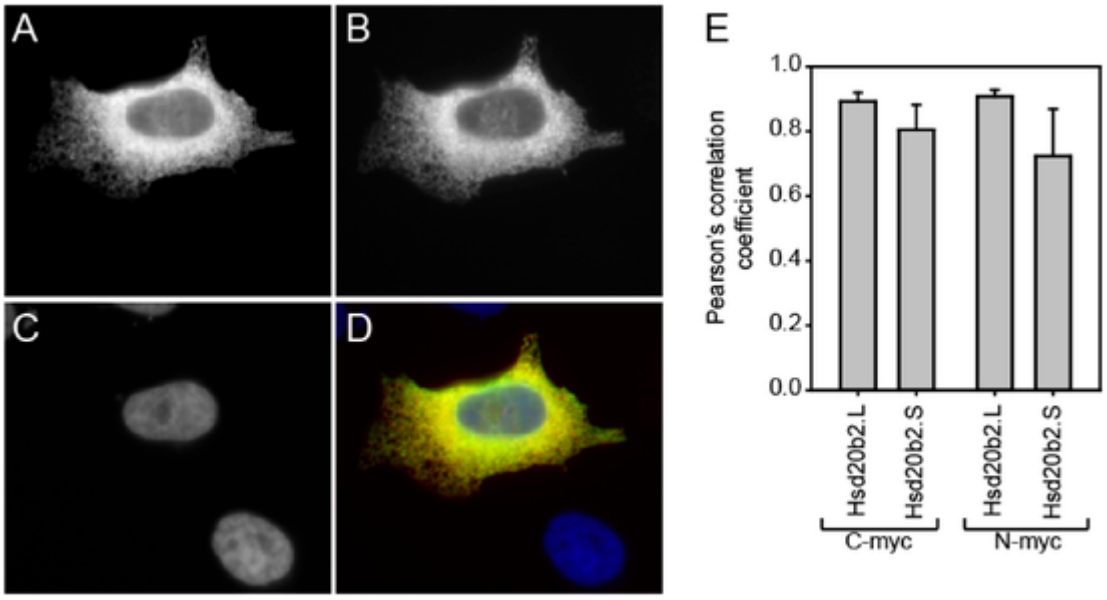

Fig. 4. Analyses of subcellular localization of *X. laevis* 20β-HSD type 2 homeologs showed that both enzymes co-localize with the endoplasmic reticulum. Panels A-D show representative images for Hsd20b2.L. The panels depict the detection of recombinant N-terminally myc-tagged Hsd20b2.L by anti-myc-antibody (A), the endoplasmic reticulum by DsRed expression (B), and the nuclei by Hoechst 33342 staining (C), and the overlay of all panels (D). Magnification: 630 × . Panel E summarizes the Pearson's correlation coefficients of co-localization of the respective 20β-HSD type 2 homeolog with the marker for the endoplasmic reticulum as mean with standard deviation based on 10 images per construct.

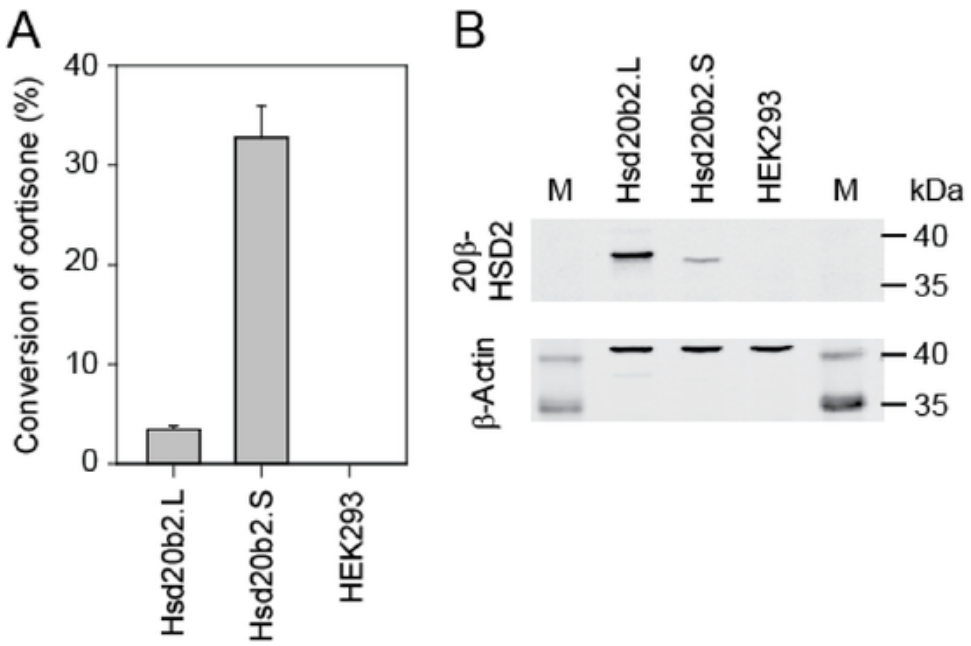

Fig. 5. Both *X. laevis* 20β-HSD type 2 homeologs catalyzed the conversion of cortisone to 20β-dihydrocortisone and are expressed in transfected HEK293 cells. 140 μg of total protein per reaction were incubated with tritiated cortisone for 15 min at 23 °C (n = 3). Cortisone conversion (shown as mean with standard deviation) was observed in transfected cells, but not in untransfected control cells (A). Visualization of recombinant expression of C-terminally myc-tagged 20β-HSD type 2 homeologs in HEK293 cells by Western Blot (B). 10 μg of total protein were separated by SDS-PAGE. β-Actin (at ~ 41 kDa) and recombinant 20β-HSD type 2 enzymes (~ 38 kDa) were detected by anti-β-actin and anti-C-myc antibodies, respectively, on the same blot using the Li-Cor Odyssey imaging system. The complete Western blot is shown in Supplementary Fig. 4. M, molecular weight marker.

Table 1
Kinetic constants of *X. laevis* 20β-HSD type 2 homeologs.

Enzyme	Apparent K_M (μM)	Apparent v_{max} (pmol min^{-1} mg^{-1} total protein)
Hsd20b2.L	20.7 ± 4.1	89.9 ± 8.9
Hsd20b2.S	3.8 ± 0.6	166.4 ± 12.9

Fig. 1. The conversion of cortisone by Hsd20b2.S being greater than by Hsd20b2.L (Fig. 5 A) can be explained by the lower K_M and the higher v_{max} for Hsd20b2.S, although Hsd20b2.S expression levels were lower.

3.5. Screen for additional steroidal substrates using LC-MS/MS

Teleost 20β-HSD type 2 enzymes possess multispecificity by catalyzing the conversion of a range of C_{21} steroids [22]. Thus, we analyzed whether the *X. laevis* 20β-HSD type 2 isoforms are able to catalyze the 20β-reduction of several different steroids from the glucocorticoid biosynthesis pathway, namely 17α-hydroxyprogesterone, progesterone, 11-deoxycortisol, 11-deoxycorticosterone, cortisol, and corticosterone. Further, we investigated if both isoforms possess 17β-HSD activity on androgens and estrogens with androstenedione and estrone as substrates. Steroid concentrations were used in physiological ranges. Experiments were conducted in triplicates from three different cell batches, each batch being an independent experiment consisting of four individually transfected cell culture flasks. Western Blot showed similar expression of recombinant proteins in individual culture flasks of each cell batch (Supplementary Fig. 2). As observed before (Fig. 5 A), Hsd20b2.L showed stronger expression than Hsd20b2.S (Supplementary Fig. 2).

The *X. laevis* 20β-HSD type 2 homeologs performed the 20β-reduction on several substrates. Both Hsd20b2.L and Hsd20b2.S catalyzed the conversion of 17α-hydroxyprogesterone to 17α,20β-dihydroxyprogesterone and converted nearly all substrate under the given conditions (Fig. 6 A). Progesterone was almost completely reduced to 20β-hydroxyprogesterone by Hsd20b2.S, but to a lesser extent by Hsd20b2.L (Fig. 6 B). As observed previously [22], the untransfected HEK293 cells converted a small proportion of progesterone into an unknown metabolite not included in our LC–MS/MS method, visible in a lower progesterone concentration measured in untransfected cells compared to the input samples. 11-Deoxycortisol was accepted as substrate by both *X. laevis* 20β-HSD type 2 homeologs. Hsd20b2.S converted almost all 11-deoxycortisol to 20β-dihydro-11-deoxycortisol, while Hsd20b2.L converted only roughly 50 % of the substrate (Fig. 6 C). Also 11-deoxycorticosterone was almost completely reduced to 20β-dihydro-11-deoxycorticosterone by Hsd20b2.S; however, Hsd20b2.L catalyzed the conversion of this steroid only barely (Fig. 6 D).

Hsd20b2.S, but not Hsd20b2.L, converted both active glucocorticoid hormones cortisol and corticosterone to their corresponding 20β-reduced metabolites (Fig. 6 E, F). In comparison to the other C_{21} steroids that were mostly completely reduced by Hsd20b2.S, the enzyme catalyzed the reduction of cortisol and corticosterone only very weakly.

Our investigation of the 17β-hydroxysteroid dehydrogenase activity revealed that both Hsd20b2.L and Hsd20b2.S produced small amounts of estradiol when incubated with the substrate estrone (Fig. 6 G). Although the measured product concentration was extremely low, the product formation was significantly different from the background of untransfected HEK293 cells (Supplementary Fig. 3). In contrast, neither Hsd20b2.L nor Hsd20b2.S converted androstenedione to testosterone (Fig. 6 H).

In none of the analytical runs, side products beside the expected products were observed.

4. Discussion

In several teleosts and mammals, 20β-HSD type 2 enzymes are known, and some members of this enzyme family have been characterized in detail [18,19,21,22]. Here, we report the identification of three new members of this family derived from the African clawed frog, *X. laevis*, and the Western clawed frog, *X. tropicalis*. We also report the

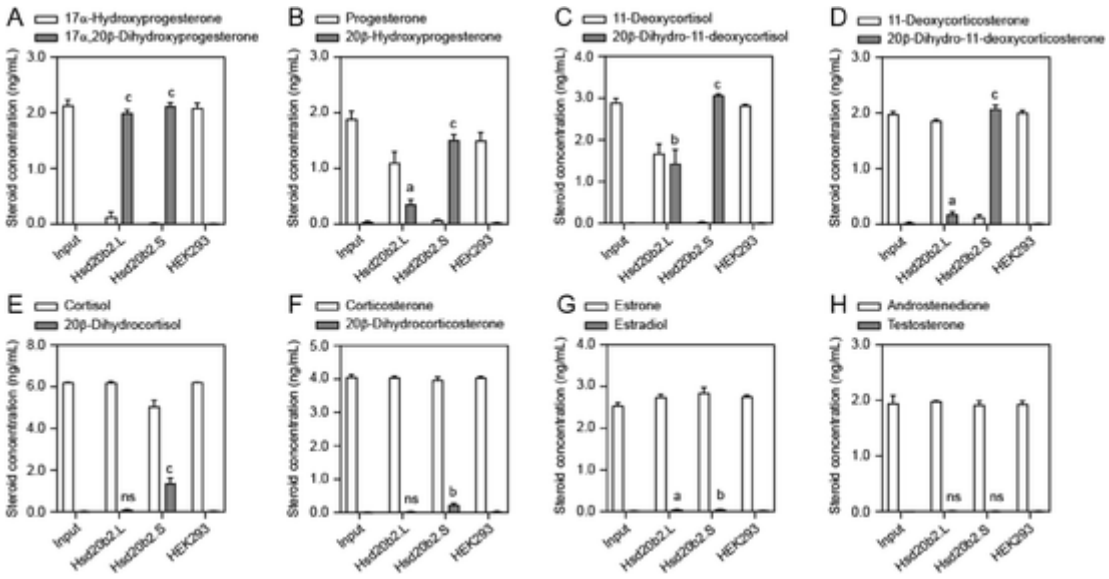

Fig. 6. Enzymatic assays with *X. laevis* 20β-HSD type 2 homeologs with eight steroid substrates revealed substrate multispecificity. 200 μg of total protein of HEK293 cells, either transfected for expression of 20β-HSD type 2 enzymes or untransfected, were incubated with the substrates 17α-hydroxyprogesterone (A), progesterone (B), 11-deoxycortisol (C), 11-deoxycorticosterone (D), cortisol (E), corticosterone (F), estrone (G), or androstenedione (H) and the cofactor NADPH. LC-MS/MS was used to quantify substrates and products. Steroid concentrations are shown as mean values from triplicates of three different cell batches (n = 9) with standard deviations. Data for substrates are presented in white bars and those for the corresponding products in gray bars. Data for individual replicates are shown in Supplementary Table 5. Single lowercase letters indicate a statistically significant difference in product formation between transfected and untransfected HEK293 cells: a, p-value between 0.01 and 0.001; b, p-value between 0.001 and 0.0001; c, p-value below 0.0001; ns, not significant. Note that the catalytic activities of Hsd20b2.L and Hsd20b2.S cannot be compared directly, because the expression levels of the enzymes differed (Supplementary Fig. 2).

characterization of the two homeologs from *X. laevis*. Our study is thus the first description of amphibian 20β-HSD type 2 enzymes.

4.1. X. laevis Hsd20b2 homeologs and their ortholog X. tropicalis Hsd20b2 fit into the 20β-HSD type 2 enzyme family

By phylogenetic analysis, the five identified 20β-HSD type 2 candidate sequences in the genome of *X. laevis* and *X. tropicalis* could be grouped into distinct clusters of 20β-HSD type 2, 17β-HSD type 12, and 17β-HSD type 3 enzymes. In all three clusters, the frog sequences were located between the teleost and the mammalian sequences, reflecting the vertebrate evolutionary lineage. The N-terminus of *X. tropicalis* 20β-HSD type 2 was noticeably longer than the ones of zebrafish and *X. laevis* 20β-HSD type 2 enzymes. This implies the presence of at least two start codons that might entail alternative translation start sites in this sequence [35]. The two 20β-HSD type 2 candidate sequences from *X. laevis* were mapped to the individual subgenomes of *X. laevis*, giving rise to the names Hsd20b2.L and Hsd20b2.S. Thus, the genes *hsd20b2.L* and *hsd20b2.S* belong to the proportion of genes that were retained in two homeologous copies in the allotetraploid genome of the frog [5].

Functional characterization of candidate 20β-HSD type 2 enzymes was conducted only for the *X. laevis* homeologs, because we had no access to *X. tropicalis* tissue samples. The co-localization of both *X. laevis* 20β-HSD type 2 enzymes with the endoplasmic reticulum is similar to that of teleost and mammalian 20β-HSD type 2 enzymes that are also associated with this compartment [18], presumably being anchored in the ER membrane with an N-terminal transmembrane helix like 17β-HSD type 3 [36]. The expression pattern of the *X. laevis* genes *hsd20b2.L* and *hsd20b2.S* is remarkably similar to the expression pattern of teleost *hsd20b2*. Zebrafish *hsd20b2* was found with strongest signals in liver, kidney (including the interrenal), intestine, gonads, and gills [18], and *hsd20b2* from Japanese eel showed strong expression in liver, testis, and pituitary [19]. Zebrafish *hsd20b2* was maternally provided to the oocyte and showed expression throughout the embryonic development [18]. In *X. laevis*, *hsd20b2.S* and to a lesser extent also *hsd20b2.L* were present in stage 0, indicating maternal provision of both transcripts to the oocyte. Both *X. laevis* Hsd20b2.L and Hsd20b2.S catalyzed the conversion of cortisone to 20β-dihydrocortisone. This reaction is also catalyzed by all characterized teleost orthologs from zebrafish, guppy, rainbow trout, and tilapia [18,22]. Whether the 20β-HSD type 2 from Japanese eel also catalyzes the 20β-reduction of cortisone has not been analyzed so far [19].

The newly identified *X. tropicalis* 20β-HSD type 2 fits well into the family of 20β-HSD type 2 enzymes from teleost fish and mammals based on sequence analyses alone. For the *X. laevis* Hsd20b2.L and Hsd20b2.S, we could show that they integrate into this family not only by high sequence identity but also by similar subcellular localization, the catalysis of the 20β-reduction of cortisone, and the comparable tissue expression pattern.

4.2. Cortisone is no physiological substrate for X. laevis Hsd20b2.L and Hsd20b2.S

X. laevis Hsd20b2.L showed less 20β-reduction of cortisone than Hsd20b2.S under identical reaction conditions, although Western blot analysis revealed that Hsd20b2.L was more strongly expressed than Hsd20b2.S. Similar deviations between expression level and activity were observed for other teleost and mammalian 20β-HSD type 2 enzymes as well [22]. However, the 20β-reduction of cortisone by *X. laevis* 20β-HSD type 2 enzymes is most likely not a physiological reaction happening *in vivo*. Two lines of evidence support this hypothesis. First, our determination of kinetic parameters with Hsd20b2.L and Hsd20b2.S with the substrate cortisone revealed very high K_M values in the μM range (20.7 μM and 3.8 μM, respectively). It is unlikely that such high cortisone concentrations appear in a living organism, and thus, both enzymes would catalyze the 20β-reduction *in vivo* at suboptimal velocities. Second, 17α-hydroxylated glucocorticoids such as 11-deoxycortisol, cortisol, and cortisone seem to be absent in *X. laevis*. When whole kidneys containing interrenal cells of *X. laevis* tadpoles were incubated with ^{14}C-labelled progesterone, the downstream metabolites corticosterone and aldosterone were found in large quantities, but cortisol was never detected [37]. In humans, 17α-

hydroxylated glucocorticoids arise from 17α-hydroxyprogesterone, which is an intermediate steroid in the conversion of progesterone to androstenedione [15]. The two-step reaction from progesterone to androstenedione is catalyzed by cytochrome P450 enzyme CYP17 (P450c17, gene symbol CYP17A1), which first 17α-hydroxylates progesterone yielding 17α-hydroxyprogesterone and then performs the 17,20-lyase reaction on the intermediate product thus forming androstenedione [15]. However, human CYP17 has little to no 17,20-lyase activity on 17α-hydroxyprogesterone [38], and androstenedione is in humans predominantly formed from dehydroepiandrosterone (DHEA) [39]. In contrast to human CYP17, the *X. laevis* CYP17 was found to possess both 17α-hydroxylase and 17,20-lyase activity. Its 17,20-lyase activity was shown to be faster than its 17α-hydroxylase activity [38]. Furthermore, the gene *cyp17a1* is almost exclusively expressed in gonads, with stronger signals in testes than in ovaries and very low levels in other tissues [5,27,40]. Based on the gonad-focused expression of CYP17 and its strong 17,20-lyase activity, it is assumed that all 17α-hydroxyprogesterone is instantly converted to androstenedione and is not available for 21-hydroxylation by CYP21 yielding 17α-hydroxylated glucocorticoids.

4.3. *X. laevis Hsd20b2.L and Hsd20b2.S show substrate multispecificity in vitro*

Since cortisone is most likely not the physiological substrate for both Hsd20b2.L and Hsd20b2.S, we performed a screen to identify more putative physiological steroidal substrates for both enzymes using our previously developed and validated LC-MS/MS method for glucocorticoids and androgens [22] as well as the method of the Stero*IDQ* kit for estrogens [33]. This approach allowed the evaluation of both 17β- and 20β-HSD activity of *X. laevis* Hsd20b2.L and Hsd20b2.S *in vitro*.

The absence of 17β-HSD activity of both enzymes with the substrate androstenedione is consistent with our previous data observed for teleost and mammalian 20β-HSD type 2 enzymes [18,22] and in line with data for tilapia 20β-HSD type 2, initially named 17β-HSD type 12 [41], showing no 17β-HSD activity with androstenedione and estrone. Interestingly, 20β-HSD type 2 from Japanese eel was able to convert 11-ketoandrostenedione to 11-ketotestosterone *in vitro* [19], suggesting that at least this member of the 20β-HSD type 2 family possesses 17β-reductive activity. Estrone to estradiol conversion might be possible for the enzyme family, because the *X. laevis* 20β-HSD type 2 enzymes had a minor 17β-reductive activity on the substrate estrone. However, this small product formation was only visible by our sensitive LC-MS/MS set-up and would have been missed with other methodologies such as thin-layer chromatography or UV-HPLC. However, due to the very small estradiol formation, we believe that the 17β-reductive activity of Hsd20b2.L and Hsd20b2.S is not relevant *in vivo* in *X. laevis*.

Both Hsd20b2.L and Hsd20b2.S had a strong 20β-HSD activity on the C_{21} steroids progesterone, 17α-hydroxyprogesterone, 11-deoxycorticosterone, and 11-deoxycortisol. Most of these steroids were converted to a lesser extent by Hsd20b2.L, with the exception of 17α-hydroxyprogesterone that was almost equally converted by both enzymes. The active glucocorticoid hormones corticosterone and cortisol were only weakly converted by Hsd20b2.S, but not by Hsd20b2.L. This is in accordance to our findings with teleost 20β-HSD type 2 enzymes [22] and might be explained by the bulky hydroxyl group at C11 (which is the common feature of cortisol and corticosterone) that cannot be easily incorporated into the active site of the enzyme. As we used C_{21} steroid concentrations in the low nanomolar range in our *in vitro* assays, the observed reactions are likely to occur *in vivo* as well.

Taken together, both 20β-HSD type 2 enzymes from *X. laevis* show substrate multispecificity, as we observed previously for the teleost and mammalian 20β-HSD type 2 enzymes [22]. The question whether *X. laevis* 20β-HSD type 2 enzymes are only multispecific or promiscuous needs to be unraveled in future research. Substrate multispecificity, the enzymes' ability to catalyze the same chemical transformation on several different substrates, is common for most enzymes [42,43]. Substrate promiscuity is present if the enzyme converts structurally very distinct substrates [42]. Among hydroxysteroid dehydrogenases, substrate promiscuity is common, because several members convert not only steroidal substrates but also prostaglandins, fatty acids with different chain lengths, retinoids, and bile acids [17,44,45].

4.4. *Involvement of X. laevis Hsd20b2 isoforms in oocyte maturation is unlikely*

In vitro, several teleost 20β-HSD type 2 enzymes are able to produce the maturation inducing steroid (MIS) [22], which is either 17α,20β-dihydroxy-4-pregnen-3-one (DHP, or 17,20β-P, or 17α,20β-dihydroxyprogesterone) or 17α,20β,21-trihydroxy-4-pregnen-3-one (20β-S, or 20β-dihydro-11-deoxycortisol) depending on the species [46,47]. The MIS induces germinal vesicle breakdown, spindle formation, chromosome condensation, and first polar body formation [47]. It is a vital hormone for oocyte maturation in teleost fish [47]. For most known teleost 20β-HSD type 2 enzymes, the involvement in MIS formation *in vivo* was not yet demonstrated. Only in masu salmon (*Oncorhynchus masou*), the MIS biosynthesis might be ascribed to a 20β-HSD type 2 ortholog. In this species, an enzyme named 17β-HSD type 12-like was discovered that catalyzed the formation of 17α,20β-dihydroxyprogesterone from 17α-hydroxyprogesterone [48]. Its mRNA was increased in follicles during final oocyte maturation [48]. Since we believe that this enzyme is actually a member of the 20β-HSD type 2 family [22], this would be the first evidence of a potential 20β-HSD type 2 enzyme involved in oocyte maturation.

Progesterone itself, or any of its hydroxylated metabolites, is in contrast to teleost fish not actively involved in oocyte maturation in *X. laevis*, although it was long believed to be [49]. Progesterone, as well as other steroids such as pregnenolone or DHEA, trigger oocyte maturation in isolated oocytes embedded into follicular cells [50,51]. However, thorough research established that androgens are the physiological mediators of oocyte maturation [52]. Androgens were equally or more potent activators of *X. laevis* oocyte maturation than progesterone and were more abundant in serum and ovaries of frogs stimulated with human chorionic gonadotropin [52]. The effect of progesterone or pregnenolone inducing oocyte maturation was explained by a two-cell model consisting of both follicular cells and the oocyte itself that convert the precursors progesterone and pregnenolone into the active androgen testosterone [38,49]. Since C_{21} steroids themselves are not involved in oocyte maturation and both *X. laevis* 20β-HSD type 2 enzymes did not catalyze the conversion of androstenedione to testosterone, an involvement of 20β-HSD type 2 enzymes in this process seems unlikely. However, the 20β-reduced C_{21} steroids formed by *X. laevis* 20β-HSD type 2 enzymes may have yet unknown roles in oocyte maturation.

4.5. *Potential role for Hsd20b2.L and Hsd20b2.S in steroid catabolism of X. laevis*

In humans, steroid catabolism is a two-phasic process that increases the water solubility of the molecule and facilitates its efficient excretion. The first phase alters biological activity and modifies functional groups, which then serve as conjugation targets with glucuronides and/or sulfates in the second phase [39]. Steroid catabolism is largely located in the liver, but most peripheral tissues also possess the required enzymes for steroid activation and inactivation [39]. Humans excrete steroids mostly *via* bile or urine [39]. In teleost fish, steroid catabolism is supposed to follow similar pathways as in humans, although fish possess an additional excretion route *via* the gills [53,54]. Even less is known about steroid catabolism and steroid excretion routes in *X. lae-*

vis. However, since *X. laevis* and humans share a high degree of evolutionary conservation in terms of biochemical pathways and physiological processes [1], it is assumed that steroid catabolism occurs along similar lines.

Zebrafish 20β-HSD type 2 together with 11β-HSD type 2 catalyze the formation of 20β-dihydrocortisone *via* cortisone from cortisol [21]. 20β-Dihydrocortisone was present in both free and conjugated form in large amounts in zebrafish holding water, underlining the importance of 20β-HSD type 2 in inactivation and removal of the potent stress hormone cortisol [21]. The multispecificity of teleost and frog 20β-HSD type 2 enzymes might imply a general involvement of this enzyme family in phase 1 of steroid catabolism, *i.e.*, inactivating the steroid and modifying its functional group at C20 for subsequent conjugation. The 20β-reduction increases the hydrophilicity of the steroid molecule, thus facilitating glucuronidation or sulfation. 20β-Dihydro-C_{21} steroids were identified in human urine [55,56], in mouse urine [57], and in bile of rainbow trout [58,59]. In *X. laevis*, there is no published evidence on a profile of excreted C_{21} steroids available. Yet, the expression pattern of both *hsd20b2.L* and *hsd20b2.S* with strong signals in liver, kidney, and intestine support a role for both enzymes in steroid catabolism. Both genes were also strongly expressed in the skin of both sexes. Since the skin of developing and adult frogs is permeable to small compounds [1,11,60], the 20β-HSD type 2 enzymes might act as a front-line detoxification mechanism by converting active steroid hormones taken up by the skin to inactive steroid hormones to prevent undesired steroid action.

4.6. *X. laevis Hsd20b2 isoforms may be involved in pheromone biosynthesis*

The excretion of steroids, both free and conjugated, can have additional roles besides removing unneeded hormones. Aquatic vertebrates such as fish and frogs, but also terrestrial vertebrates, use excreted compounds as pheromones for communication, which influence several behaviors such as mating, aggression, or predator avoidance [61]. Steroids are information-rich molecules that can convey information on willingness to mate or health status among conspecifics [61], as well as on kin recognition in hierarchies or school forming [62], and can synchronize gamete maturation and spawning interaction [63]. In teleost fish, reproductive pheromones are often free or conjugated steroid molecules that elicit reproductive behavior in both sexes [64]. For example, sulfated 17α,20β-dihydroxyprogesterone induced reproductive behavior in goldfish and zebrafish [63,65], while roach (*Rutilus rutilus*) responded to free and glucuronidated 17α,20β-dihydroxyprogesterone among other steroids [66]. *X. laevis* tadpoles detected a variety of sulfated pregnane-based steroids, while non-sulfated steroids in most cases failed to activate the sulfated steroid-responsive neurons [67]. 20β-Hydroxylated C_{21} steroids were not tested for their stimulatory potential so far. Those steroids tested, namely free corticosterone, free cortisone, and cortisol-21-sulfate, elicited no response in tadpoles [67]. However, tadpole and frog breeding water contained a variety of sulfated steroids capable of activating sulfated steroid-responsive neurons [67]. Unfortunately, the identities of these sulfated steroids were not determined [67].

The information about intraspecies communication *via* pheromones in frogs is limited [67], as is the information on the identity of involved steroid molecules. Therefore, it is possible that both 20β-HSD type 2 variants of *X. laevis* are involved in the biosynthesis of molecules that can act after possible conjugations as pheromones. Since both enzymes are expressed already during embryonic development, a role of their reaction products as reproductive pheromones seems less likely than a role in sensing conspecifics. Yet, the function of possible reaction products might as well change during development and adulthood of the frogs. Further research is needed to elucidate whether *X. laevis* 20β-HSD type 2 enzymes are important pheromone synthesizing enzymes.

5. Conclusion

Our work shows a detailed characterization of two novel 20β-HSD type 2 enzymes from *X. laevis* and the identification of their ortholog in *X. tropicalis*. It is thus the first description of 20β-HSD type 2 enzymes in amphibians. The expression pattern, subcellular localization, and enzymatic activity of *X. laevis* 20β-HSD type 2 is comparable to previously characterized members from the 20β-HSD type 2 family, with whom the enzymes also share a high degree of identity. Both *X. laevis* 20β-HSD type 2 enzymes showed substrate multispecificity by catalyzing the 20β-reduction of several C_{21} steroids, which is in accordance to other teleost 20β-HSD type 2 enzymes and common among hydroxysteroid dehydrogenases. Both frog 20β-HSD type 2 homeologs might play a role in steroid catabolism by converting active steroid hormones to inactive metabolites dedicated for further conjugation and removal from the organism. A role for both enzymes in pheromone biosynthesis for intraspecies communication is also possible, whereas an involvement in oocyte maturation is less likely. The actual physiological role of both 20β-HSD type 2 homeologs in *X. laevis* remains to be elucidated for example by generating knock-down animals and characterizing their physiology in detail.

CRediT authorship contribution statement

Janina Tokarz: Conceptualization, Methodology, Formal analysis, Investigation, Writing - original draft. **Stefan M. Schmitt:** Methodology, Writing - review & editing. **Gabriele Möller:** Conceptualization, Writing - review & editing. **André W. Brändli:** Funding acquisition, Writing - review & editing. **Jerzy Adamski:** Supervision, Funding acquisition, Writing - review & editing.

Declaration of Competing Interest

The authors have no conflicts of interest to disclose.

Acknowledgements

We are grateful to Gabriele Zieglmeier and Marion Schieweg for technical assistance with cell culture and activity assays. We acknowledge the help of Madlaina von Hößlin and Lena Djermester with cloning the coding sequences. We thank Maria Kugler and Dr. Jutta Lintelmann for help with the measurement of estrogens. A.W.B. was supported by a grant from the European Commission (EU FP7 Program, EURenOmics Grant Agreement 305608).

Appendix A. Supplementary data

Supplementary material related to this article can be found, in the online version, at doi:https://doi.org/10.1016/j.jsbmb.2021.105874.

References

[1] S.M. Schmitt, M. Gull, A.W. Brändli, Engineering Xenopus embryos for phenotypic drug discovery screening, Adv. Drug Deliv. Rev. 69–70 (2014) 225–246, https://doi.org/10.1016/j.addr.2014.02.004.
[2] R.M. Harland, R.M. Grainger, Xenopus research: metamorphosed by genetics and genomics, Trends Genet. 27 (2011) 507–515, https://doi.org/10.1016/j.tig.2011.08.003.
[3] D. Bhattacharya, C.A. Marfo, D. Li, M. Lane, M.K. Khokha, CRISPR/Cas9: An. inexpensive, efficient loss of function tool to screen human disease genes in Xenopus, Dev. Biol. 408 (2015) 196–204, https://doi.org/10.1016/j.ydbio.2015.11.003.
[4] I.M. Grant, D. Balcha, T. Hao, Y. Shen, P. Trivedi, I. Patrushev, J.D. Fortriede, J.B. Karpinka, L. Liu, A.M. Zorn, P.T. Stukenberg, D.E. Hill, M.J. Gilchrist, The Xenopus ORFeome: a resource that enables functional genomics, Dev. Biol. 408 (2015) 1–13, https://doi.org/10.1016/j.ydbio.2015.09.004.
[5] A.M. Session, Y. Uno, T. Kwon, J.A. Chapman, A. Toyoda, S. Takahashi, et al., Genome evolution in the allotetraploid frog Xenopus laevis, Nature 538

(2016) 336–343, https://doi.org/10.1038/nature19840.
[6] R.E. Kälin, N.E. Bänziger-Tobler, M. Detmar, A.W. Brändli, An in vivo chemical library screen in Xenopus tadpoles reveals novel pathways involved in angiogenesis and lymphangiogenesis, Blood. 114 (2009) 1110–1122, https://doi.org/10.1182/blood-2009-03-211771.
[7] D. Raciti, L. Reggiani, L. Geffers, Q. Jiang, F. Bacchion, A.E. Subrizi, D. Clements, C. Tindal, D.R. Davidson, B. Kaissling, A.W. Brändli, Organization of the pronephric kidney revealed by large-scale gene expression mapping, Genome Biol. 9 (2008), https://doi.org/10.1186/gb-2008-9-5-r84.
[8] D.R. Buchholz, More similar than you think: frog metamorphosis as a model of human perinatal endocrinology, Dev. Biol. 408 (2015) 188–195, https://doi.org/10.1016/j.ydbio.2015.02.018.
[9] Y. Katsu, S. Kohno, K. Oka, M.E. Baker, Evolution of corticosteroid specificity for human, chicken, alligator and frog glucocorticoid receptors, Steroids. 113 (2016) 38–45, https://doi.org/10.1016/j.steroids.2016.06.005.
[10] Y. Katsu, K. Oka, M.E. Baker, Evolution of human, chicken, alligator, frog, and zebrafish mineralocorticoid receptors: allosteric influence on steroid specificity, Sci. Signal. 11 (2018) 35–37, https://doi.org/10.1126/scisignal.aao1520.
[11] S. Bissegger, M.A. Pineda Castro, V. Yargeau, V.S. Langlois, Phthalates modulate steroid 5-reductase transcripts in the Western clawed frog embryo, Comp. Biochem. Physiol. Part - C Toxicol. Pharmacol. 213 (2018) 39–46, https://doi.org/10.1016/j.cbpc.2018.07.005.
[12] M. Hecker, J.W. Park, M.B. Murphy, P.D. Jones, K.R. Solomon, G. Van Der Kraak, J.A. Carr, E.E. Smith, L. du Preez, R.J. Kendall, J.P. Giesy, Effects of atrazine on CYP19 gene expression and aromatase activity in testes and on plasma sex steroid concentrations of male African clawed frogs (Xenopus laevis), Toxicol. Sci. 86 (2005) 273–280, https://doi.org/10.1093/toxsci/kfi203.
[13] W. Kloas, I. Lutz, Amphibians as model to study endocrine disrupters, J. Chromatogr. A 1130 (2006) 16–27, https://doi.org/10.1016/j.chroma.2006.04.001.
[14] R. Poulsen, X. Luong, M. Hansen, B. Styrishave, T. Hayes, Tebuconazole disrupts steroidogenesis in Xenopus laevis, Aquat. Toxicol. 168 (2015) 28–37, https://doi.org/10.1016/j.aquatox.2015.09.008.
[15] W.L. Miller, R.J. Auchus, The molecular biology, biochemistry, and physiology of human steroidogenesis and its disorders, Endocr. Rev. 32 (2010) 1–71, https://doi.org/10.1210/er.2010-0013.
[16] F. Hu, E.J. Crespi, R.J. Denver, Programming neuroendocrine stress axis activity by exposure to glucocorticoids during postembryonic development of the frog, Xenopus laevis, Endocrinology 149 (2008) 5470–5481, https://doi.org/10.1210/en.2008-0767.
[17] G. Moeller, J. Adamski, Integrated view on 17beta-hydroxysteroid dehydrogenases, Mol. Cell. Endocrinol. 301 (2009) 7–19, https://doi.org/10.1016/j.mce.2008.10.040.
[18] J. Tokarz, R. Mindnich, W. Norton, G. Möller, M. Hrabé de Angelis, J. Adamski, Discovery of a novel enzyme mediating glucocorticoid catabolism in fish: 20beta-Hydroxysteroid dehydrogenase type 2, Mol. Cell. Endocrinol. 349 (2012) 202–213, https://doi.org/10.1016/j.mce.2011.10.022.
[19] H. Suzuki, Y. Ozaki, S. Ijiri, K. Gen, Y. Kazeto, 17β-Hydroxysteroid dehydrogenase type 12a responsible for testicular 11-ketotestosterone synthesis in the Japanese eel, Anguilla japonica, J. Steroid Biochem. Mol. Biol. 198 (2020) 105550, https://doi.org/10.1016/j.jsbmb.2019.105550.
[20] L. Xiao, Y. Guo, D. Wang, M. Zhao, X. Hou, S. Li, H. Lin, Y. Zhang, Beta-hydroxysteroid dehydrogenase genes in orange-spotted grouper (Epinephelus coioides): genome-wide identification and expression analysis during sex reversal, Front. Genet. 11 (2020) 1–11, https://doi.org/10.3389/fgene.2020.00161.
[21] J. Tokarz, W. Norton, G. Möller, M. Hrabé de Angelis, J. Adamski, Zebrafish 20β-hydroxysteroid dehydrogenase type 2 is important for glucocorticoid catabolism in stress response, PLoS One 8 (2013) e54851, https://doi.org/10.1371/journal.pone.0054851.
[22] J. Tokarz, J. Lintelmann, G. Möller, J. Adamski, Substrate multispecificity among 20β-hydroxysteroid dehydrogenase type 2 members, Mol. Cell. Endocrinol. 510 (2020) 110822, https://doi.org/10.1016/j.mce.2020.110822.
[23] A. Anitha, Y.R. Gupta, S. Deepa, M. Ningappa, K.B. Rajanna, B. Senthilkumaran, Gonadal transcriptome analysis of the common carp, Cyprinus carpio: identification of differentially expressed genes and SSRs, Gen. Comp. Endocrinol. 279 (2019) 67–77, https://doi.org/10.1016/j.ygcen.2018.12.004.
[24] S. Kumar, G. Stecher, K. Tamura, MEGA7: Molecular Evolutionary Genetics Analysis Version 7.0 for Bigger Datasets, Mol. Biol. Evol. 33 (2016) 1870–1874, https://doi.org/10.1093/molbev/msw054.
[25] N. Saitou, M. Nei, The neighbor-joining method: a new method for reconstructing phylogenetic trees, Mol. Biol. Evol. 4 (1987) 406–425, https://doi.org/10.1093/oxfordjournals.molbev.a040454.
[26] J. Felsenstein, Confidence Limits On Phylogenies: An Approach Using the Bootstrap, Evolution (N. Y). 39 (1985) 783–791, https://doi.org/10.1111/j.1558-5646.1985.tb00420.x.
[27] K. Karimi, J.D. Fortriede, V.S. Lotay, K.A. Burns, D.Z. Wang, M.E. Fisher, T. J. Pells, C. James-Zorn, Y. Wang, V.G. Ponferrada, S. Chu, P. Chaturvedi, A. M. Zorn, P.D. Vize, Xenbase: A genomic, epigenomic and transcriptomic model organism database, Nucleic Acids Res. 46 (2018) D861–D868, https://doi.org/10.1093/nar/gkx936.
[28] S.F. Altschul, T.L. Madden, A.A. Schäffer, J. Zhang, Z. Zhang, W. Miller, D.J. Lipman, Gapped BLAST and PSI-BLAST: a new generation of protein database search programs, Nucleic Acids Res. 25 (1997) 3389–3402, https://doi.org/10.2503/jjshs.58.977.
[29] S.F. Altschul, J.C. Wootton, E.M. Gertz, R. Agarwala, A. Morgulis, A.A. Schäffer, Y. Yu, Protein database searches using compositionally adjusted substitution matrices, FEBS J. 272 (2005) 5101–5109.
[30] A.W. Brändli, M.W. Kirschner, Molecular cloning of tyrosine kinases in the early Xenopus embryo: identification of eck-related genes expressed in cranial neural crest cells of the second (Hyoid) Arch, Dev. Dyn. 203 (1995) 119–140, https://doi.org/10.1002/aja.1002030202.
[31] P.D. Nieuwkoop, J. Faber, Normal Table of Xenopus laevis (Daudin): a Systematical and Chronological Survey of the Development from the Fertilized Egg Till the End of Metamorphosis, North-Holland Publishing Company, Amsterdam, 1956.
[32] M.M. Bradford, A rapid and sensitive method for the quantitation of microgram quantities of protein utilizing the principle of protein-dye binding, Anal. Biochem. 72 (1976) 248–254, https://doi.org/10.1016/0003-2697(76)90527-3.
[33] T. Koal, D. Schmiederer, H. Pham-Tuan, C. Röhring, M. Rauh, Standardized LC-MS/MS based steroid hormone profile-analysis, J. Steroid Biochem. Mol. Biol. 129 (2012) 129–138, https://doi.org/10.1016/j.jsbmb.2011.12.001.
[34] U. Oppermann, C. Filling, M. Hult, N. Shafqat, X. Wu, M. Lindh, J. Shafqat, E. Nordling, Y. Kallberg, B. Persson, H. Jornvall, Short-chain dehydrogenases/reductases (SDR): the 2002 update, Chem. Biol. Interact. 143–144 (2003) 247–253.
[35] A.V. Kochetov, Alternative translation start sites and hidden coding potential of eukaryotic mRNAs, BioEssays. 30 (2008) 683–691, https://doi.org/10.1002/bies.20771.
[36] M. Tsachaki, A. Odermatt, Subcellular localization and membrane topology of 17β-hydroxysteroid dehydrogenases, Mol. Cell. Endocrinol. 489 (2019) 98–106, https://doi.org/10.1016/j.mce.2018.07.003.
[37] G. Jolivet-Jaudet, J. Leloup-Hatey, Interrenal function during amphibian metamorphosis: in vitro biosynthesis of radioactive corticosteroids from (414C)-progesterone by interrenal in Xenopus laevis tadpoles, Comp. Biochem. Physiol. Part B Biochem. 79 (1984) 239–244, https://doi.org/10.1016/0305-0491(84)90020-8.
[38] W.H. Yang, L.B. Lutz, S.R. Hammes, Xenopus laevis ovarian CYP17 is a highly potent enzyme expressed exclusively in oocytes: evidence that oocyte play a critical role in Xenopus ovarian androgen production, J. Biol. Chem. 278 (2003) 9552–9559, https://doi.org/10.1074/jbc.M212027200.
[39] L. Schiffer, L. Barnard, E.S. Baranowski, L.C. Gilligan, A.E. Taylor, W. Arlt, C.H.L. Shackleton, K.-H. Storbeck, Human steroid biosynthesis, metabolism and excretion are differentially reflected by serum and urine steroid metabolomes: a comprehensive review, J. Steroid Biochem. Mol. Biol. 194 (2019) 105439, https://doi.org/10.1016/j.jsbmb.2019.105439.
[40] R.P. Piprek, M. Damulewicz, M. Kloc, J.Z. Kubiak, Transcriptome analysis identifies genes involved in sex determination and development of Xenopus laevis gonads, Differentiation. 100 (2018) 46–56, https://doi.org/10.1016/j.diff.2018.02.004.
[41] L.Y. Zhou, D.S. Wang, B. Senthilkumaran, M. Yoshikuni, Y. Shibata, T. Kobayashi, C.C. Sudhakumari, Y. Nagahama, Cloning, expression and characterization of three types of 17beta-hydroxysteroid dehydrogenases from the Nile tilapia, Oreochromis niloticus, J. Mol. Endocrinol. 35 (2005) 103–116, https://doi.org/10.1677/jme.1.01801.
[42] W.M. Atkins, Biological messiness vs. Biological genius: mechanistic aspects and roles of protein promiscuity, J. Steroid Biochem. Mol. Biol. 151 (2015) 3–11, https://doi.org/10.1016/j.jsbmb.2014.09.010.
[43] S.D. Copley, Shining a light on enzyme promiscuity, Curr. Opin. Struct. Biol. 47 (2017) 167–175, https://doi.org/10.1016/j.sbi.2017.11.001.
[44] F. Haller, E. Moman, R.W. Hartmann, J. Adamski, R. Mindnich, Molecular framework of steroid/retinoid discrimination in 17beta-hydroxysteroid dehydrogenase type 1 and photoreceptor-associated retinol dehydrogenase, J. Mol. Biol. 399 (2010) 255–267, https://doi.org/10.1016/j.jmb.2010.04.002.
[45] G. Moeller, J. Adamski, Multifunctionality of human 17beta-hydroxysteroid dehydrogenases, Mol. Cell. Endocrinol. 248 (2006) 47–55, https://doi.org/10.1016/j.mce.2005.11.031.
[46] E. Clelland, C. Peng, Endocrine/paracrine control of zebrafish ovarian development, Mol. Cell. Endocrinol. 312 (2009) 42–52, https://doi.org/10.1016/j.mce.2009.04.009.
[47] Y. Nagahama, M. Yamashita, Regulation of oocyte maturation in fish, Dev. Growth Differ. 50 (Suppl 1) (2008) 195–219, https://doi.org/10.1111/j.1440-169X.2008.01019.x.
[48] S. Ijiri, Y. Shibata, N. Takezawa, Y. Kazeto, N. Takatsuka, E. Kato, S. Hagihara, Y. Ozaki, S. Adachi, K. Yamauchi, Y. Nagahama, 17b-HSD type 12-Like is responsible for maturation-inducing hormone synthesis during oocyte maturation in Masu Salmon, Endocrinology. 158 (2017) 627–639, https://doi.org/10.1210/en.2016-1349.
[49] S.R. Hammes, Steroids and oocyte maturation - A new look at an old story, Mol. Endocrinol. 18 (2004) 769–775, https://doi.org/10.1210/me.2003-0317.
[50] O. Haccard, A. Dupré, P. Liere, A. Pianos, B. Eychenne, C. Jessus, R. Ozon, Naturally occurring steroids in Xenopus oocyte during meiotic maturation. Unexpected presence and role of steroid sulfates, Mol. Cell. Endocrinol. 362 (2012) 110–119, https://doi.org/10.1016/j.mce.2012.05.019.
[51] S. Schorderet-Slatkine, Action of progesterone and related steroids on oocyte

maturation in Xenopus laevis. An in vitro study, Cell Differ. 1 (1972) 179–189.
[52] L.B. Lutz, L.M. Cole, M.K. Gupta, K.W. Kwist, R.J. Auchus, S.R. Hammes, Evidence that androgens are the primary steroids produced by Xenopus laevis ovaries and may signal through the classical androgen receptor to promote oocyte maturation, Proc. Natl. Acad. Sci. U. S. A. 98 (2001) 13728–13733, https://doi.org/10.1073/pnas.241471598.
[53] T.P. Mommsen, M.M. Vijayan, T.W. Moon, Cortisol in teleosts: dynamics, mechanisms of action, and metabolic regulation, Rev. Fish Biol. Fish. 9 (1999) 211–268.
[54] E.L. Vermeirssen, A.P. Scott, Excretion of free and conjugated steroids in rainbow trout (Oncorhynchus mykiss): evidence for branchial excretion of the maturation-inducing steroid, 17,20 beta-dihydroxy-4-pregnen-3-one, Gen. Comp. Endocrinol. 101 (1996) 180–194, https://doi.org/10.1006/gcen.1996.0020.
[55] B. Eisenschmid, P. Heilmann, W. Oelkers, R. Rejaibi, M. Schöneshöfer, 20-Dihydroisomers of cortisol and cortisone in human urine: excretion rates under different physiological conditions, J. Clin. Chem. Clin. Biochem. 25 (1987) 345–349 http://www.ncbi.nlm.nih.gov/pubmed/3625132.
[56] M. Schöneshöfer, B. Weber, W. Oelkers, K. Nahoul, F. Mantero, Measurement of urinary free 20 alpha-dihydrocortisol in biochemical diagnosis of chronic hypercorticoidism., Clin. Chem. 32 (1986) 808–810 http://www.ncbi.nlm.nih.gov/pubmed/3009052.
[57] C.H.L. Shackleton, B.A. Hughes, G.G. Lavery, E.A. Walker, P.M. Stewart, The corticosteroid metabolic profile of the mouse, Steroids. 73 (2008) 1066–1076, https://doi.org/10.1016/j.steroids.2008.04.004.
[58] T.G. Pottinger, T.A. Moran, P.A. Cranwell, The biliary accumulation of corticosteroids in rainbow trout, Oncorhynchus mykiss, during acute and chronic stress, Fish Physiol. Biochem. 10 (1992) 55–66.
[59] B. Truscott, Steroid metabolism in fish - identification of steroid moieties of hydrolyzable conjugates of cortisol in the bile of trout Salmo gairdnerii, Gen. Comp. Endocrinol. 38 (1979) 196–206.
[60] X. Jia, Z. Liu, X. Lu, J. Tang, Y. Wu, Q. Du, J. He, X. Zhang, J. Jiang, W. Liu, Y. Zheng, Y. Ding, W. Zhu, H. Zhang, Effects of MCLR exposure on sex hormone synthesis and reproduction-related genes expression of testis in male Rana nigromaculata, Environ. Pollut. 236 (2018) 12–20, https://doi.org/10.1016/j.envpol.2018.01.057.
[61] W.I. Doyle, J.P. Meeks, Excreted steroids in vertebrate social communication, J. Neurosci. 38 (2018) 3377–3387, https://doi.org/10.1523/JNEUROSCI.2488-17.2018.
[62] P.W. Sorensen, N.E. Stacey, Brief review of fish pheromones and discussion of their possible uses in the control of non-indigenous teleost fishes, New Zeal, J. Mar. Freshw. Res. 38 (2004) 399–417, https://doi.org/10.1080/00288330.2004.9517248.
[63] N. Stacey, Hormones, pheromones and reproductive behavior, Fish Physiol. Biochem. 28 (2003) 229–235.
[64] N. Stacey, P. Sorensen, Reproductive pheromones, Fish Physiol. 24 (2005) 359–412, https://doi.org/10.1016/S1546-5098(05)24009-8.
[65] R. van den Hurk, W.G. Schoonen, G. a van Zoelen, J.G. Lambert, The biosynthesis of steroid glucuronides in the testis of the zebrafish, Brachydanio rerio, and their pheromonal function as ovulation inducers., Gen. Comp. Endocrinol. 68 (1987) 179–188 http://www.ncbi.nlm.nih.gov/pubmed/3428552.
[66] N. Lower, A.P. Scott, A. Moore, Release of sex steroids into the water by roach, J. Fish Biol. 64 (2004) 16–33, https://doi.org/10.1046/j.1095-8649.2003.00278.x.
[67] A. Sansone, T. Hassenklöver, T. Offner, X. Fu, T.E. Holy, I. Manzini, Dual processing of sulfated steroids in the olfactory system of an anuran amphibian, Front. Cell. Neurosci. 9 (2015) 1–10, https://doi.org/10.3389/fncel.2015.00373.